standard deviation $\sigma_i(\theta_i)$ in accordance with the equipartition theorem is equal to:

$$\sigma_i(\theta_i) = \sqrt{\frac{K_B T \theta_i^2}{2E_g(\theta)}}\,.$$

When tension in a nicked DNA molecule is increased to 65 pN, it displays a reversible, cooperative transition to an extended form that is approximately 70 % longer than normal *B*-DNA and with a substantially reduced twist. It was also found the twist-stretch coupling in these molecules. Evidence exists that overstreched DNA (polynucleotide) may present one of the following structures: (i) base-paired (dubbed *S* form, doubbed-helix) or (ii) two independent strands of ssDNA which are similar in structure (*see* B. Bhushan, ed., 2004) to polypeptide single helix (Fig. 8-11b).

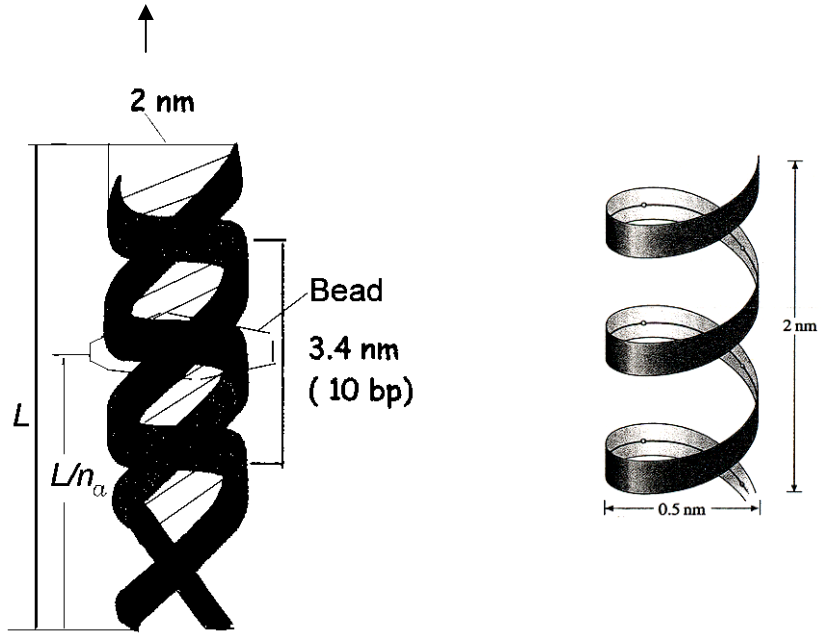

Fig. 8-11. Helico

Helicoidal model. We assume now that the stretched DNA model (i) in the mechanical aspects is similar to the elastic helicoid (Fig. 8-11a) made of a punched pretwisted strip and model (ii) is similar (Fig. 8-11b) to a coiled ribbon structure (*see* Chap. 4). Let us consider the features of base-paired structure (i). For twist-stretch coupling $D_c = M/F_Q$ estimation, we can use modified conditional radius formula (4-79) of elastic pretwisted strip $D_C = \rho_C = \dfrac{j_{k\tau} - j_{\tau\tau} i_{\theta m}}{j_{kk} - j_{\tau k} i_{\theta m}}$, (8-19)

where $j_{\tau\tau} = GT_0(1+\nu_{ipf} b_1^2 k_p^2/\lambda)$; $j_{kk} = EA$; $i_{\theta m} = \dfrac{Ek_p}{4n_a G\lambda}(1+\nu_{ipf} b_1^2 k_p^2/\lambda)^{-1}$, and

$j_{k\tau}=j_{\tau k}=EAb_1^2k_p/4.$

Here $j_{k\tau}=j_{\tau k}$ is the tension stiffness of a pretwisted strip under its tension with a simultaneous twist or the stiffness of this strip under its twist with a simultaneous tension, $j_{\tau\tau}$ is the twist stiffness of a pretwisted strip under twist with an applied torque, but without tension, j_{kk} is the tension stiffness of the pretwisted strip under tension without twist, $i_{\theta m}=|\theta/(sn_a)|$ is modified ratio in rad/nm between the untwist angle θ and corresponding stretch s of the pretwisted strip, and n_a=1-2 is a factor of the experimental submicrometer rotor bead location on the DNA molecule with $1/n_a$ as a length fraction (*see* Fig. 8-11a and J. Gore *et al*., *Nature* **442**, 836, 2006).

Any elastic mechanical model requires knowledge of its constituents' mechanical properties, particularly Young's modulus and Poisson's ratio of the material. In DNA case, we have specifics in this regard. Some researchers present the experimental equivalent to Young's modulus value by the stretch modulus of DNA F_{stm}= 1,000-1,100 pN, which is expressed as a force value. Meanwhile, Young's modulus E should be expressed as a stress value: $E=F_{stm}/A_{cDNA}$, where A_{cDNA} is the conditional area of DNA's model cross section. For example, 1) $A_{cDNA1}=\pi d_D^2/4$ for the model with the round elastic rod of diameter d_D, 2) $A_{cDNA2}=(b_o\times h_o-\pi b_{1i}\times h_{1i})$ for the model with the pretwisted hollow nanostrip (Fig. 8-12a), where $b_{o,i}=2b_{1o,i}$ are the widths and $h_{oi}=2h_{1o,i}$ are the thickness of the outer (index $_o$) rectangular and inner (index $_i$) elliptical cross sections, respectively. Hence, the equivalent Young's modulus E_e can have different values. Let us recall that DNA conditional "diameter" d_D in the model 1) is usually equal to 2-2.2 nm which corresponds to E_{e1}= 346-350 pN/nm^2= 3.46-3.5× 10^8 Pa (*see* S.B. Smith *et al*., 1996). We accept for the model 2) b_o=2.1 nm or as approximately equal to DNA cell diameter, h_o=0. 295 nm, b_i=1.75 nm, h_i=0.22 nm (Fig. 8-12a), and A_{cDNA2} = 0.317 nm^2. Therefore E_{e2}= 3470 pN/nm^2. Please note that the product $E_eA_c=F_{stm}\approx$ 1,000-1,100 pN remains the same for both models. Poisson's ratio is usually accepted equal to ν_p=0.5. Let us also denote $\lambda=(h_o/b_o)^2=0.0197$; the ratio between elastic moduli $\nu_{E/G}=E/G=2(1+\nu_p)$, and ratio between the section torsional stiffness T_0 and area A_c magnitude as

$$\nu_{T_0/A}=T_0/A_c=\{0.3333\,b_o^4\lambda^{3/2}-[(\pi/16)b_i^4\lambda^{3/2}/(1+\lambda)]\}/A_{cDNA\,2}=0.04\ \text{nm}^2.$$

Substituting all of these expressions into (19), we obtain, after corresponding cancellations, the final formula for the twist-stretch DNA coupling calculation as follows

$$D_c=\frac{(k_{p0}/4)[b_1^2-n_a^{-1}\nu_{T_0/A}\lambda^{-1}]}{1-(b_1^2k_{p0}^2/16n_a)\nu_{E/G}(\lambda+\nu_{ipf}b_1^2k_{p0}^2)^{-1}}. \qquad (8\text{-}20)$$

Calculations with this formula well correspond to DNA experimental data. For example, D_c=0.087 nm or $F_{stm}D_c=g_D\approx$90 pN· nm at n_a=1.65 and accepted parameters of our DNA model. In accordance with Table 7-3, the limit of statistical fluctuations' standard deviation for the pretwisted strip structure is equal to:

$$\sigma_{\varepsilon M}=\sqrt{\frac{k_BTL(\lambda+\nu_{ipf}\,b_1^2k_{p0}^2)}{EA(\lambda+0.18\,b_1^2k_{p0}^2)}}. \qquad (8\text{-}21)$$

Note that (21) corresponds to the equipartition theorem.
Let us recall that k_BT=4.1 pN·nm is the product of Boltzmann's constant and the absolute temperature T=293 K. We also can assume that for double-stranded DNA the expression $EA\,(\lambda+0.18\,b_{1o}^2k_{p0}^2)/L(\lambda+\nu_{if}pb_{1o}^2k_{p0}^2)\approx F/s$ is a stretch stiffness (*see* experimental data in C. Bustamante *et al*., 2003; T. Strunz *et al*., 1999; and A. Sarkar *et al*., 2001; *see* also DNA precision assembler options in *Nature*, **459**, 414, 2009).

Persistence length in our model is equal to $A_{bp}=E_{e2}J_\eta/\,[\sqrt{2}\;(k_BT)]$=51 nm,

where E_{e2}=3470 pN/nm^2, $J_\eta=\frac{1}{2}(J_{\eta\,o}-J_{\eta\,i})\approx(b_o^3h_o/24)-(\pi b_{1i}^3h_{1i}/128)$ =0.085 nm^4 is the moment of inertia for the hollow cross section of a pretwisted strip. Similar values of the DNA persistence length 50-53 nm are shown in many published sources. A mean experimental value at different cases for A_{bp} =(30+80)/2=55 nm.

We estimate the **stretch force-untwist rotation** angle (F-θ) function of the pretwisted nanostrip by the following formula (Table 4-8): $\theta=F\,j_\theta^{-1}$. (8-22)
We can estimate the spring stiffness k_h of DNA hydrogen bonds as a product of the translational s and rotational θ motion transformation i_θ= θ/s and the torsional rigidity at the pretwisted strip extension $j_\theta=F/\theta$, which yields

$$k_h=\frac{EA(1+\nu_{jf}\chi_{kp})}{L_b(1+\nu_{if}\chi_{kp})}=1{,}131.6\ \text{pN/nm},$$

where ν_{jf}=0.14 is the rigidity factor for the rectangular cross section, ν_{if}=0.41is the transformation factor for the perforated pretwisted strip, $\chi_{kp}=k_{p0}^2(b_o/2)^2\lambda^{-1}$ =190.9, and L_b=0.34 nm is the length of one DNA bones' base pair.

Overwinding option for DNA model can be caused by the decrease $2\Delta b_o$ of the strip's cross section width by negative stress σ^{11} (*see* Fig. 8-12a and p.80) with

$$\Delta b_O=-(9/112)\frac{k_{p0}^2R^2\sigma_0^{33}R}{(\lambda+0.179k_{p0}^2R^2)E_{e2}}\ , \qquad (8\text{-}23)$$

where $\sigma_0^{33}=F_{str}/A_{cDNA2}$ is the average stress of the longitudinal tension with applied force F_{str} and $R=b_o/2$. The overwinding can continue until the compression stress σ^{11} reaches the compressive yield stress for the model's anisotropic material as in the elastic coupling at plasticity limit, which occurs at F_{str}=30 pN (*see* J. Gore *et al*., Nature **442**, 836, 2006, where this experimental force value is shown, but the reason of ultimate nature for the phenomenon is not explained).

The critical point between the option to overwind and unwind the pretwisted strip under tension can be found from the equality of additional turns $2\pi(N_{01}\text{-}N_0)$ in radians and unwinding $F_{str}/\,j_\theta$ options also in radians:

$$2\pi(N_{01}\text{-}N_0)=\frac{k_{p0}L\ \ (9/112)k_{p0}^3R^3\sigma_0^{33}}{(\lambda+0.179k_{p0}^2R^2)E_{e2}}=F_{str}/\,j_\theta=\frac{2(1+\nu_p)Lk_{p0}\sigma_0^{33}}{57.3E_{e2}(\lambda+\nu_{jf}k_{p0}^2R^2)}\,, \qquad (8\text{-}24)$$

where $N_0=L/S_0$ and $N_{01}=L/(S_0-2\pi\Delta b_o)$ are the corresponding number of turns.
As a result, the critical point for the equal options of overwinding and unwinding of the strip under initial tension after certain cancellations yields the relation

$$k_{p0}^3 R^3 = \frac{224\,(1+\nu_p)}{57.3\times 9}. \qquad (8\text{-}25)$$

Let us recall that $1/(k_{p0}R) = S_0/2\pi R = \tan\alpha$, where α is a helix line angle to the cross section plane. Hence, we have found in (25) the relationship between the critical helix angle $\alpha_c = \tan^{-1}(1/(k_{p0}R))$ and the Poisson's ratio ν_p of the strip's material. Solution of (25) with ν_p=0.5 yields α_c=0.856 rad. A helix with angle $\alpha<\alpha_c$ has more probable options for overwinding at initial stretch while a helix with angle $\alpha>\alpha_c$ has a good probability to unwind under the longitudinal tension. In DNA molecule case, $\alpha=\tan^{-1}(3.4/(2\pi\,1.05))=0.476$ rad $< \alpha_c$. Hence, DNA molecule has probable option for initial overwinding. Similar conclusions about the overwinding of DNA molecule and its critical helix angle as a function of Poisson's ratio are shown in J. Gore *et al*. Nature **442**, 836,17 August, 2006, but with some difference in the critical numerical value of $\alpha_{c1}=\tan^{-1}(\sqrt{\nu_p})= 0.62$ rad. However, this difference is not very important for our DNA model with $\alpha<\alpha_{c1}$ as well.

In the case of the pretwisted bronze microstrip mechanism with ν_p=0.279,for example, the critical helix angle is equal to α_c=0.822 rad and for typical pretwisted microstrip with the cross section's width $2R$=0.12 mm and the helix pitch of S_0=2 mm $\alpha= \tan^{-1}(2/2\pi 0.06)= 1.38$ rad $> \alpha_c$ and α_{c1}. Therefore, the helicoidal mechanism with the metallic pretwisted strip has good options to unwinding under longitudinal tension and less or no options for spontaneous overwinding.

Nonlinear model. Nonlinear unwinding and thermomechanical length fluctuation variance $Var(L_c)$ of DNA molecules were found in the experimental studies at "remeasuring the double helix"(*see* R.S. Mathew-Fenn *et al*., Science **322**, 448-449, 17 October, 2008). Our model with the pretwisted nanostrip reflects those options as well. These fluctuations correspond to normal statistical distribution and in agreement with the equipartition theorem (*see* p. 298).

Hence, $Var(L_c) = \aleph k_B T / j_s$, (8-26)

where $\aleph$=157 is the factor of relations between measurement units in the left and right side of the formula in our calculations bellow with 1 nm^2=10^2 Å^2 and 1.57θ=1rad (57.295 angular degree).

We derive an equation for the nanostrip stretch nonlinear stiffness j_s as the product of nonlinear average transformation ratio $i_{\theta av}$ [*see* Eq.(2-56)] and the torsional rigidity at the pretwisted strip extension j_θ (*see* p.76). The inverse value of nonlinear stiffness j_s^{-1} therefore is equal to:

$$j_s^{-1} = \frac{L_c[1+\nu_{if}(1+\nu_H)^2\chi_{kp}+3(1+\nu_H)\nu_H\chi_{kp}/8]}{E_{e2}[(1+\nu_H)+\nu_H-3k_{p0}^2(1+\nu_H)^2\nu_H b_{1o}^2](1+\nu_{jf}\chi_{kp})A_{cDNA2}}, \qquad (8\text{-}27)$$

where ν_{if}=0.39-0.41and ν_{jf}=0.18 are the transformation form coefficients for the hollow(perforated) strip, parameters $\nu_H=-\theta/k_{p0}L_c<0$ and θ are the stretched strip moving end's rotation relative and absolute angles, respectively. Values of the parameter ν_H are inversely proportional to the molecule length L_c if the angle θ=constant. Therefore, $\nu_{Hi}/\nu_{Hj} = L_{cj}/L_{ci}$. (8-28)

Table 8-12 shows results of our calculations with application of (26), (27) and (28) equations and accepting ν_H (L_c=131.1 Å)=-0.15. The difference, δ %, between thus calculated and experimental values is less than 10%. These data are also represented

in Fig. 8-12b where solid line reflects the calculated results and circles correspond to the experimental values. Our calculations with (26) show that nonlinear variance for the molecule of length 50 nm at ν_H =-0.039 is about two times larger than for linear relations.

Table 12. Thermomechanical variance of DNA molecule's length

N $\frac{O}{—}$	Calculation (26), (27), (28)				Experiment *		δ (%)
	ν_H	ν_{lf}	L_c (Å)	*Var* (Å^2)	L_c (Å)	*Var* (Å^2)	
1	-0.35	0.41	56.4	8.4	56.4	8.7	3.4
2	-0.228	0.39	86.1	22.5	86.1	21.2	6.1
3	-0.194	0.39	103.4	27.9	103.4	28.4	1.8
4	-0.167	0.39	121.4	43.4	121.4	42.4	2.4
5	-0.15	0.39	131.1	51.5	131.1	49.4	4.2

* After R.S. Mathew-Fenn *et al*., Science **322**, 448-449 (2008), idem. ibid. PloS One **3**, e3229 (2008)

a) b)

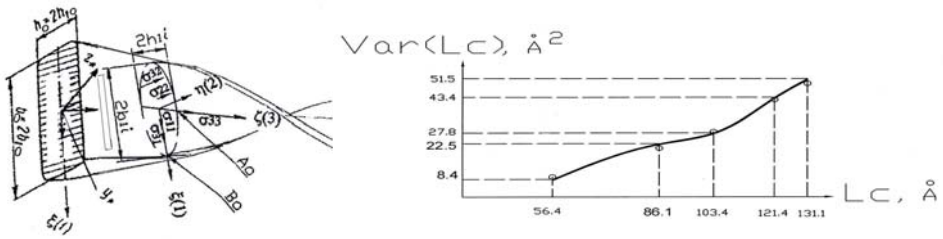

Fig. 8-12. Pretwisted hollow nanostrip (a) and its length thermomechanical variance (b) with calculated functions in solid line and experimental data in circles.

The twisting of stretched DNA can lead to other structural transitions. For example, after a critical amount of overwinding has been introduced into a molecule, it may buckle. Complex force-extension curves with multiple force plateaus are seen when single DNA molecules are twisted in either direction and pulled to high forces. This allows us to assume possible jumps of hysteresis asymmetry at a fast and slow extension and the relaxation of the DNA molecules similar to those in the pretwisted helicoids (see Chap. 5). The developed model allows us study DNA mechanics in more comprehensive way. Particularly, it explains why overwinding stops at application of 30 pN extension force to DNA molecule. We derived on this model's basis the unknown previously specific analytical nonlinear function of DNA length thermomechanical variance, which corresponds with a good accuracy to the experimental data. Of course, all these assumptions and the described elastic helicoidal model's application to DNA mechanics should be experimentally verified and theoretically developed in more detail. This experimental verification is still very difficult as a result of the ultimately small sizes and acting forces. However, the closeness of biomechanics and precision nano-elastic mechanics is evident.

Problem 4. Free V-shaped cantilever parallel beam approximation (PBA) is studied and accepted by many researchers (*see* H.-J. Butt *et al*.,1993; J.E. Sader , 1995, *RSI* **66**, 4583). This model, however, has the following specific nodal points position equation on the constituent rectangular beams ("legs") with length *L* and unit length mass *m* at higher resonance modes:

$$\frac{J_M(\alpha L)^3 U(\alpha L) - T(\alpha L) - \varepsilon(\alpha L) S(\alpha L)}{S(\alpha L) + (\alpha L)\varepsilon V(\alpha L) - J_M(\alpha L)^3 T(\alpha L)} U(\alpha x) + V(\alpha x) = 0 \text{ ,} \quad (8\text{-}29)$$

where $J_M = J_0/mL^3$, J_0 is the moment of rotational inertia V-shaped cantilever's extended mass M_{ad} of triangular (trapezoid) part with an offset L_{of} of its center of gravity beyond a moving end of the constituent beams, and $\varepsilon = L_{of}/L$. One can see that this equation will be the same as (8-4a) if J_M=0 and ε=0. In addition, a rectangular cantilever with end extended mass has the following (*see* B.R. Bhat, H. Wagner, J. Sound Vib.,1976,**45**, 304) frequency equation (8-30):

$$1 + C_F + \alpha_M A_1 (R_F - P_F) - 2\alpha_M (A_1)^2 \varepsilon H_F - (J_M + \alpha_M \varepsilon^2)(A_1)^3 (R_F + P_F) + J_M (A_1)^4 \alpha_M (1 - C_F) = 0,$$

where $A_1 = (\alpha L)_n$; $C_F = \cosh A_1 \cos A_1$; $R_F = \sinh A_1 \cos A_1$; $P_F = \cosh A_1 \sin A_1$; $H_F = \sinh A_1 \sin A_1$, $\alpha = \sqrt[4]{m\omega^2/EJ}$ is the frequency factor, and mass factor $\alpha_M = M_{ad}/mL$.

After the constituent beams' mutual skew θ cosine function evaluation $n_k = 1/(\cos^4(\theta/2))$, we can easily estimate V-shaped cantilever's relative increase of spring constants $K_{vn}/K_{v1} = n_k K_{n1}$ at higher oscillation modes ω_n with the known rectangular constituent beam's spring constants (for the same modes) increase $K_{n1} = K_n/K_1$, which can be determined on the basis of the force superposition (kinetostatic) method (*see* section 8-4 and Y.M. Tseytlin, *Rev. Sci. Instrum*. **79**, 025102, 2008) using equations (29) and (30).

Further research in the structural synthesis of precision elastic chains may be directed to the more effective elastic correctors, study of mechanical motion in the quantum regime, simplification of enough accurate analytical methods for new effective elastic systems synthesis in the field of micro- and nano-scale, and improvement of their metrological traceability, especially in the area of nanotechnology, picometer, femto-Joule, subattogram - zeptogram, and subattonewton detection, including detection of tiny chemical, biological agents, and vapor molecules (*see* N.V. Lavrik *et al*., 2004). Thorough research should be performed on new, more stable, non-corrosive elastic materials and films with negligible internal damping, increased range of a linear stress-strain relationships, larger endurance and tensile stress limits, lesser temperature expansion coefficients, lesser density, larger modulus of elasticity, larger *MYS*, and better "machinability". Special research is now intensified on new methods and materials for the fabrication of nonplanar spiral and helical microstructures with DNA, carbon nanocoils which may be the most sensitive mechanical transformers of micro-motion, joining elastic links by laser and electron ray welding without softening or cracking the elastic material, cold bonding setting with resins and adhesives [e.g., advanced Araldite, Yacca gum resin with E=5 GPa, Elmer's glue with E=0.6 GPa (*see* X. Chen *et al*., 2004; S.W. Schediwy *et al*., 2005)], and effective mechanical clamping. A new and promising option is the growing of carbon nanotube's tips and super-sharp (tip radius 1-2 nm) tungsten nanowire directly on the atomic force microscopy cantilever's movable end with probe and depositing fine-crystalline diamond particles grown on standard silicon tips that provide necessary stiffness and eliminate structural damping in these very responsible systems of highly sensitive scientific instruments. Effective growing attachment methods and synthesis of helical micro- and nano-springs include chemical-vapor deposition and electrospinning. All these problems are related to the next generation of the structural synthesis in precision elasticity.

Springer

http://www.springer.com/978-0-387-25156-1

Structural Synthesis in Precision Elasticity
Tseytlin, Y.M.
2006, XVI, 400 p. 96 illus., Hardcover
ISBN: 978-0-387-25156-1